

Trimerization of NaC_2N_3 to $\text{Na}_3\text{C}_6\text{N}_9$ in the Solid: Ab Initio Crystal Structure Determination of Two Polymorphs of NaC_2N_3 and of $\text{Na}_3\text{C}_6\text{N}_9$ from X-ray Powder Diffractometry

Barbara Jürgens,[†] Elisabeth Irran,[†] Julius Schneider,[‡] and Wolfgang Schnick^{*,†}

Department Chemie, Ludwig-Maximilians-Universität München, Butenandtstrasse 5-13 (Haus D), D-81377 Munich, Germany, and Institut für Kristallographie und Angewandte Mineralogie, Ludwig-Maximilians-Universität München, Theresienstrasse 41, D-80333 Munich, Germany

Received August 30, 1999

Sodium dicyanamide NaC_2N_3 was found to undergo two phase transitions. According to thermal analysis and temperature-dependent X-ray powder diffractometry, the transition of $\alpha\text{-NaC}_2\text{N}_3$ (**1a**) to $\beta\text{-NaC}_2\text{N}_3$ (**1b**) occurs at 33 °C and is displacive. **1a** crystallizes in the monoclinic system, space group $P2_1/n$ (no. 14), with $a = 647.7(1)$, $b = 1494.8(3)$, $c = 357.25(7)$ pm, $\beta = 93.496(1)$ °, and $Z = 4$. The structure was solved from powder diffraction data ($\text{Cu K}\alpha_1$, $T = 22$ °C) using direct methods and it was refined by the Rietveld method. The final agreement factors were $wR_p = 0.072$, $R_p = 0.053$, and $R_F = 0.074$. **1b** crystallizes in the orthorhombic system, space group $Pbnm$ (no. 62), with $a = 650.15(5)$, $b = 1495.1(2)$, $c = 360.50(3)$ pm, and $Z = 4$. The structure was refined by the Rietveld method using the atomic coordinates of **1a** as starting values ($\text{Mo K}\alpha_1$, $T = 150$ °C). The final agreement factors were $wR_p = 0.044$, $R_p = 0.034$, $R_F = 0.140$. The crystal structures of both polymorphs contain sheets of Na^+ and $\text{N}(\text{CN})_2^-$ ions which are in **1a** nearly and in **1b** exactly coplanar. Above 340 °C, **1b** trimerizes in the solid to $\text{Na}_3\text{C}_6\text{N}_9$ (**2**). **2** crystallizes in the monoclinic system, space group $P2_1/n$ (no. 14), with $a = 1104.82(1)$, $b = 2338.06(3)$, $c = 351.616(3)$ pm, $\beta = 97.9132(9)$ °, and $Z = 4$. The structure was solved from synchrotron powder diffraction data ($\lambda = 59.733$ pm) using direct methods and it was refined by the Rietveld method. The final agreement factors were $wR_p = 0.080$, $R_p = 0.059$, and $R_F = 0.080$. The compound contains Na^+ and the planar tricyanomelamine $\text{C}_6\text{N}_9^{3-}$. The phase transition from **1b** to **2** is reconstructive. It occurs in the solid-state without involvement of other phases or intermediates. The crystal structures of **1b** and **2** indicate that there is no preorientation of the $\text{N}(\text{CN})_2^-$ in the solid before their trimerization to $\text{C}_6\text{N}_9^{3-}$.

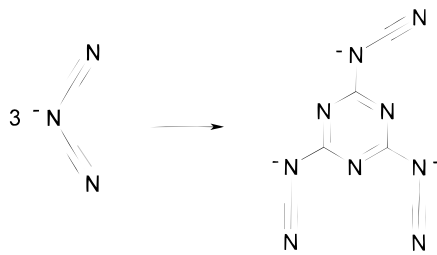
Introduction

Trimerization of molecules to compounds with a *s*-triazine ring is a well-known phenomenon in the chemistry of carbon nitrides, e.g., cyanogen chloride ClCN trimerizes to 2,4,6-trichloro-*s*-triazine (cyanuric chloride) $\text{C}_3\text{N}_3\text{Cl}_3$ and cyanamide H_2CN_2 trimerizes to 2,4,6-triamino-*s*-triazine (melamine) $\text{C}_3\text{N}_3(\text{NH}_2)_3$.¹ With regard to the synthesis of expanded C–N sheets containing the *s*-triazine ring system, detailed knowledge about the C_3N_3 ring formation is of special interest.

In 1922 Madelung et al. reported on the trimerization of dicyanamide ions $\text{N}(\text{CN})_2^-$ to tricyanomelamine ions $\text{C}_6\text{N}_9^{3-}$ by heating sodium dicyanamide NaC_2N_3 .² Purdy et al. studied the similar thermolysis of LiC_2N_3 .³

In a previous work we described the reinvestigation of Madelung's experiment by IR spectroscopy and single-crystal structure determination of the trihydrate $\text{Na}_3\text{C}_6\text{N}_9 \cdot 3\text{H}_2\text{O}$.⁴ Because structural data have not been available for NaC_2N_3 nor for anhydrous $\text{Na}_3\text{C}_6\text{N}_9$, it was an open question whether the trimerization reaction occurs in the solid or in the melt. In addition, it is conceivable that the dimer tricyanoguanidinate $\text{C}_4\text{N}_6^{2-}$ is formed during the reaction, which is well-known as monohydrate $\text{Na}_2\text{C}_4\text{N}_6 \cdot \text{H}_2\text{O}$.⁵

Sodium dicyanamide NaC_2N_3 is commercially available and is commonly used as a starting material for the syntheses of heterocyclic compounds, organic superconductors, and molecular magnets containing dicyanamide ions.^{6–10} Despite its



* To whom correspondence should be addressed (fax: +49/89 2180-7440; E-mail: wsc@cup.uni-muenchen.de).

[†] Department Chemie.

[‡] Institut für Kristallographie und Angewandte Mineralogie.

- Huthmacher, K.; Hübner, F. In *Methods of Organic Chemistry (Houben-Weyl)*, Vol. E 9 c, *Heterocycles IV*; Schaumann, E., Ed.; Thieme Verlag: Stuttgart, New York, 1998; p 667.
- Madelung, W.; Kern, E. *Liebigs Ann. Chem.* **1922**, 427, 26.
- Purdy, A.; Houser, E.; George, C. F. *Polyhedron* **1997**, 16, 3671.
- Jürgens, B.; Milius, W.; Morys, P.; Schnick, W. *Z. Anorg. Allg. Chem.* **1998**, 624, 91.
- Subrayan, R. S.; Francis, A. H.; Kampf, J. W.; Rasmussen, P. G. *Chem. Mater.* **1995**, 7, 2213.
- Chivers, T.; Gates, D.; Li, X.; Manners, I.; Parvez, M. *Inorg. Chem.* **1999**, 38, 70.
- Kini, A. M.; Geiser, U.; Wang, H. H.; Carlson, K. D.; Williams, J. M.; Kwok, W. K.; Vandervoort, K. G.; Thompson, J. E.; Stupka, D. L.; Jung, D.; Whangbo, M.-H. *Inorg. Chem.* **1990**, 29, 2555.
- Batten, S. R.; Jensen, P.; Moubaraki, B.; Murray, K. S.; Robson, R. *Chem. Commun.* **1998**, 439.
- Kurmoo, M.; Kepert, C. J. *J. New Chem.* **1998**, 2, 1515.

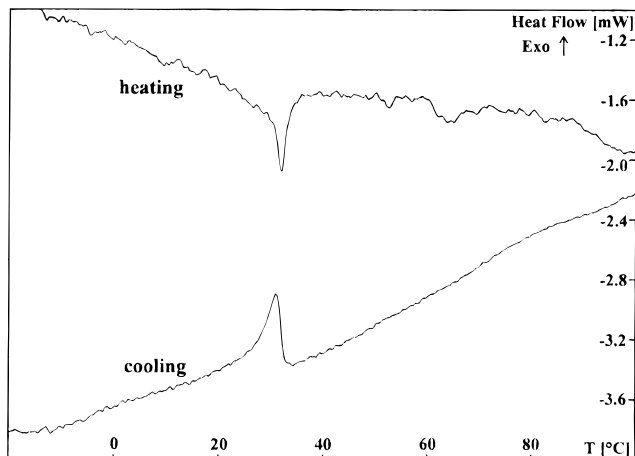


Figure 1. DSC curve of the reversible phase transition of α - to β - NaC_2N_3 (**1a**, **1b**).

importance, to date no crystal structure determination of this compound has been published.

We now report on the solid-state phase transitions of NaC_2N_3 , which are documented by thermoanalytical measurements and high-temperature X-ray diffraction. The crystal structures of α - and β - NaC_2N_3 , as well as the crystal structure of anhydrous $\text{Na}_3\text{C}_6\text{N}_9$, are determined by ab initio powder diffraction.

Experimental Section

Sodium dicyanamide NaC_2N_3 (**1**) was obtained from Fluka ($\geq 96\%$) and used without further purification.

Preparation of Trisodium Tricyanomelamine $\text{Na}_3\text{C}_6\text{N}_9$ (2**).** The compound was prepared by heating **1b** above $340\text{ }^\circ\text{C}$ in a sealed quartz ampule under argon atmosphere. The crystallinity of the obtained white powder increased significantly with increasing temperature. Accordingly, a sample obtained at $600\text{ }^\circ\text{C}$ was used for the synchrotron diffraction experiment. Above $650\text{ }^\circ\text{C}$ $\text{Na}_3\text{C}_6\text{N}_9$ decomposes. $\text{Na}_3\text{C}_6\text{N}_9$ is soluble in water; after slow evaporation at room temperature the trihydrate $\text{Na}_3\text{C}_6\text{N}_9 \cdot 3\text{H}_2\text{O}$ precipitates.

Thermal Analysis. Two differential scanning calorimetry (DSC) curves of NaC_2N_3 (sample weight: 17.298 mg) were recorded with a DSC 141 (Setaram). The first was recorded from -20 to $100\text{ }^\circ\text{C}$ (heating rate: $10\text{ }^\circ\text{C}/\text{min}$) and back. It shows an endothermic (heating) and exothermic (cooling) effect which belongs to a reversible phase transition of NaC_2N_3 at $33\text{ }^\circ\text{C}$ (Figure 1). The second DSC curve (25 – $550\text{ }^\circ\text{C}$, heating rate: $10\text{ }^\circ\text{C}/\text{min}$) shows a broad peak (onset $320\text{ }^\circ\text{C}$, max $380\text{ }^\circ\text{C}$) (Figure 2). During cooling no thermal effect occurred. Therefore, the transformation to $\text{Na}_3\text{C}_6\text{N}_9$ is irreversible.

X-ray Diffraction. X-ray powder diffraction data had to be used for the crystal structure determination because no single crystals of the compounds were obtained. The diffraction investigations were carried out in Debye–Scherrer geometry and the samples were enclosed in glass capillaries with 0.3 mm diameter. Details of the structure determinations and refinements are listed in Table 1.

α - NaC_2N_3 (1a**).** The powder diffraction data of **1a** were collected on a STOE Stadi P powder diffractometer with monochromatized $\text{Cu K}\alpha_1$ radiation. The obtained diffraction pattern was indexed by the program ITO¹¹ ($\text{FoM} = 60.2$) and the space group $P2_1/n$ was derived from the systematic extinctions. A small amount of NaCl was detected as impurity. There were 277 integrated intensities extracted by the program EXTRA¹² and used as input for the direct methods program SIRPOW¹³ which revealed the position of all atoms in the unit cell.

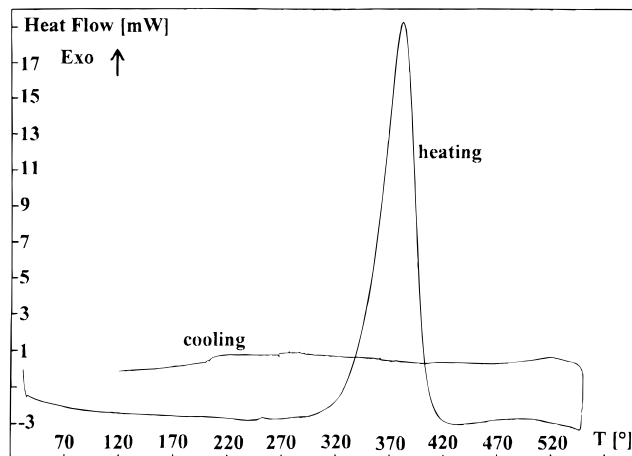


Figure 2. DSC curve of the irreversible transformation of NaC_2N_3 (**1b**) to $\text{Na}_3\text{C}_6\text{N}_9$ (**2**).

The structure was refined with the Rietveld program GSAS.¹⁴ The results of the refinement are shown in Figure 3.

β - NaC_2N_3 (1b**).** The diffraction data of **1b** were collected at $150\text{ }^\circ\text{C}$ with a STOE Stadi P powder diffractometer with monochromatized $\text{Mo K}\alpha_1$ radiation using graphite heating equipment. The pattern was indexed with lattice constants very similar to the low-temperature phase, but with an orthorhombic instead of a monoclinic unit cell. From the systematic reflection conditions the space groups $Pbn2_1$ and $Pbnm$ were considered, the latter was confirmed by the structure refinement. As starting values of the Rietveld refinement (Figure 4) the atomic coordinations of **1a** were used but with all atoms on the special Wyckoff position $4c$ (y -coordinates at $1/4$).

$\text{Na}_3\text{C}_6\text{N}_9$ (2**).** The diffraction pattern of **2** obtained on a conventional powder diffractometer (Siemens D5000, $\text{Cu K}\alpha_1$ radiation) was indexed with a monoclinic unit cell with space group $P2_1/n$, but the crystal structure could not be solved by direct methods because of the severe overlap of the diffraction peaks. Therefore, synchrotron radiation diffraction experiments were performed at the Swiss-Norwegian Beamline (BM01B) of the ESRF (Grenoble). The obtained diffraction pattern showed a much higher resolution with full width at half-maximum (fwhm) values $\Delta 2\theta < 0.02\text{ }^\circ$ at low diffraction angles. The lattice constants were confirmed ($\text{FoM} = 37.4$) and the crystal structure was solved by direct methods using EXTRA (1060 reflections) and SIRPOW. All atoms were localized by this procedure. The pattern showed an anisotropic peak broadening with [001] as broadening axis which could be fitted by the anisotropic strain model available in the program GSAS. At the beginning of the refinement all C–N distances were restrained; the theoretical values were taken from $\text{Na}_3\text{C}_6\text{N}_9 \cdot 3\text{H}_2\text{O}$.⁴ The weight of the restraints was gradually reduced and finally removed without yielding unreasonable distances. The displacement factors of all C and all N atoms, respectively, were constrained to be equal. The final results of the refinement are shown in Figure 5.

In Situ Powder Diffraction. To investigate the character of the phase transitions, temperature-dependent measurements were performed on an STOE Stadi P powder diffractometer with a computer-controlled STOE furnace in steps of $2\text{ }^\circ\text{C}$ from 16 to $50\text{ }^\circ\text{C}$ for the phase transition of **1a** to **1b** (Figure 6) and in steps of $10\text{ }^\circ\text{C}$ from 300 to $470\text{ }^\circ\text{C}$ for the transformation of **1b** to **2** (Figure 7). The heating element consists of an electrically heated graphite tube holding the sample capillary vertically with respect to the scattering plane. Bores in the graphite tube permit unobstructed pathways for the primary beam as well as for the scattered radiation. The temperature measured by a thermocouple in the graphite tube is kept constant to within $0.2\text{ }^\circ\text{C}$. The heating rate between different temperatures was set to $22\text{ }^\circ\text{C}/\text{min}$ and a waiting

- (10) Manson, J. L.; Kmety, C. R.; Huang, Q.-Z.; Lynn, J. W.; Bendele, G. M.; Pagola, S.; Stephens, P. W.; Liable-Sands, L. M.; Rheingold, A. L.; Epstein, A. J.; Miller, J. S. *Chem. Mater.* **1998**, *10*, 2552.
- (11) Visser, J. W. *J. Appl. Crystallogr.* **1969**, *2*, 89.
- (12) Altomare, A.; Burla, M. C.; Cascarano, G.; Giacovazzo, C.; Guagliardi, A.; Moliterni, A. G. G.; Polidori, G. *J. Appl. Crystallogr.* **1995**, *28*, 842.

- (13) Altomare, A.; Cascarano, G.; Giacovazzo, C.; Guagliardi, A.; Burla, M. C.; Polidori, G.; Camalli, M. *J. Appl. Crystallogr.* **1994**, *27*, 435.
- (14) von Dreele, R. B.; Larson, A. C. General Structure Analysis System. Los Alamos National Laboratory, Report LAUR 86-748; Los Alamos, NM, 1990.

Table 1. Crystallographic Data for α - NaC_2N_3 (**1a**), β - NaC_2N_3 (**1b**), and $\text{Na}_3\text{C}_6\text{N}_9$ (**2**)

	α - NaC_2N_3	β - NaC_2N_3	$\text{Na}_3\text{C}_6\text{N}_9$
M_r [g/mol]	89.03	89.03	267.10
crystal system	monoclinic	orthorhombic	monoclinic
space group	$P2_1/n$ (no. 14)	$Pbnm$ (no. 62)	$P2_1/n$ (no. 14)
powder diffractometer	STOE STADI P	STOE STADI P	BM01B/ESRF
radiation, λ [pm]	$\text{Cu K}\alpha_1$, 154.06	$\text{Mo K}\alpha_1$, 70.93	synchrotron, 59.733
temp [°C]	22	150	22
lattice constants [pm, °]	$a = 647.7(1)$ $b = 1494.8(3)$ $c = 357.25(7)$ $\beta = 93.496(1)$	$a = 650.15(5)$ $b = 1495.1(2)$ $c = 360.50(3)$ $\beta = 97.9132(9)$	$a = 1104.82(1)$ $b = 2338.06(3)$ $c = 351.616(3)$ $\beta = 97.9132(9)$
V [10^6 pm 3]	345.27(1)	350.42(5)	899.62(2)
Z	4	4	4
ρ (calc) [g/cm 3]	1.713	1.687	1.972
profile range	$3^\circ \leq 2\theta \leq 90^\circ$	$5^\circ \leq 2\theta \leq 35^\circ$	$2.5^\circ \leq 2\theta \leq 36^\circ$
no. of data points	8700	1500	6700
observed reflections	277	137	1060
atomic parameters	18	12	54
displacement factors	6	6	5
structure solution		direct methods (SIRPOW.92) ¹³	
structure refinement		Rietveld refinement (GSAS) ¹⁴	
R values	$wR_p = 0.072$ $R_p = 0.053$ $R_F = 0.074$	$wR_p = 0.044$ $R_p = 0.034$ $R_F = 0.140$	$wR_p = 0.080$ $R_p = 0.059$ $R_F = 0.080$

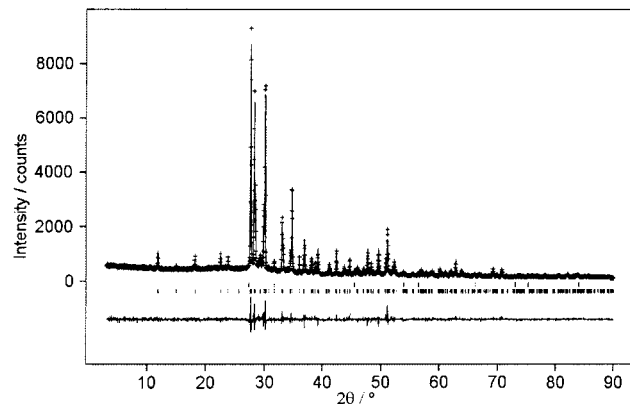


Figure 3. Observed (crosses) and calculated (line) X-ray powder diffraction pattern as well as difference profile of the Rietveld refinement of α - NaC_2N_3 (**1a**). The powder pattern was obtained with a STOE Stadi P powder diffractometer ($\lambda = 154.05$ pm).

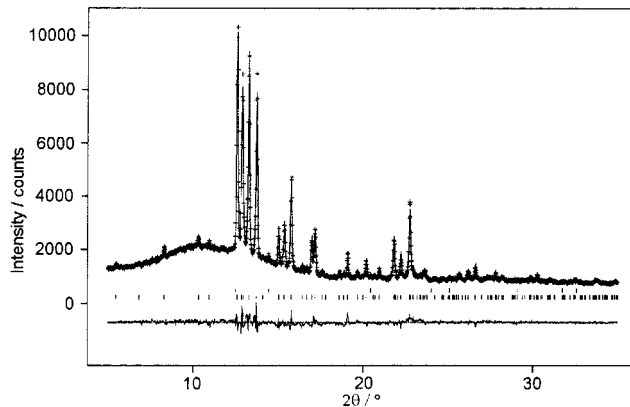


Figure 4. Observed (crosses) and calculated (line) X-ray powder diffraction pattern as well as difference profile of the Rietveld refinement of β - NaC_2N_3 (**1b**). The powder pattern was obtained with a STOE Stadi P powder diffractometer ($\lambda = 70.93$ pm).

time of 3 min was given to allow for temperature stabilization before the start of each data acquisition.

Results and Discussion

The solid **1a** is built up by $\text{N}(\text{CN})_2^-$ ions which are connected by Na^+ (Figure 8). All $\text{N}(\text{CN})_2^-$ ions are planar and are arranged

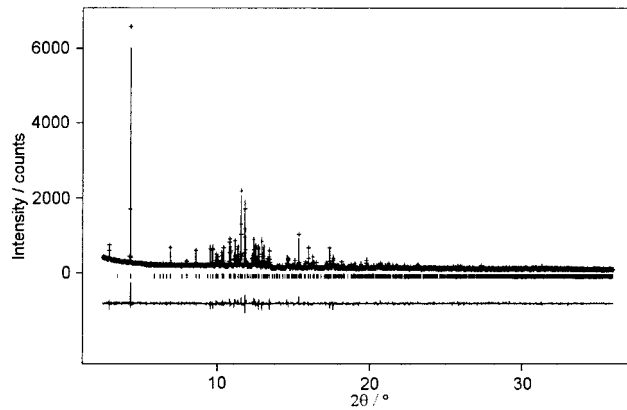


Figure 5. Observed (crosses) and calculated (line) X-ray powder diffraction pattern as well as difference profile of the Rietveld refinement of $\text{Na}_3\text{C}_6\text{N}_9$ (**2**). The powder pattern was obtained with a synchrotron source (BM01B/ESRF Grenoble, $\lambda = 59.733$ pm).

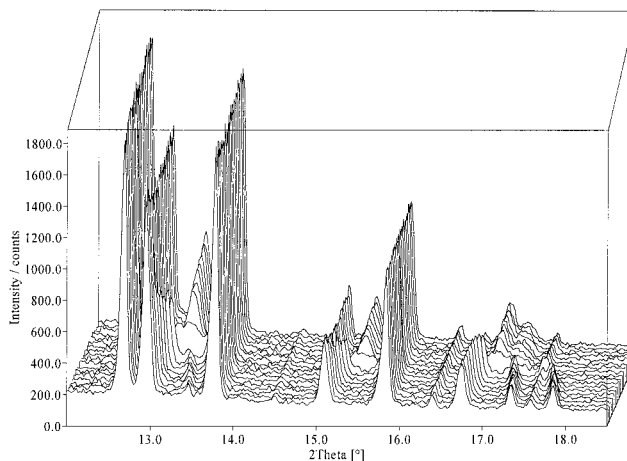


Figure 6. X-ray thermodiffractometric powder patterns of the phase transition of α - NaC_2N_3 (**1a**) to β - NaC_2N_3 (**1b**) (16–50 °C, steps 2 °C from the front to the rear).

in sheets approximately parallel (010) at about $y = 1/4$ and $3/4$ (Figure 9). The distances and angles (Table 2) of the $\text{N}(\text{CN})_2^-$ ions are comparable to those of other dicyanamides.^{8–10} The distances from the C atoms to the bridging N atoms are longer

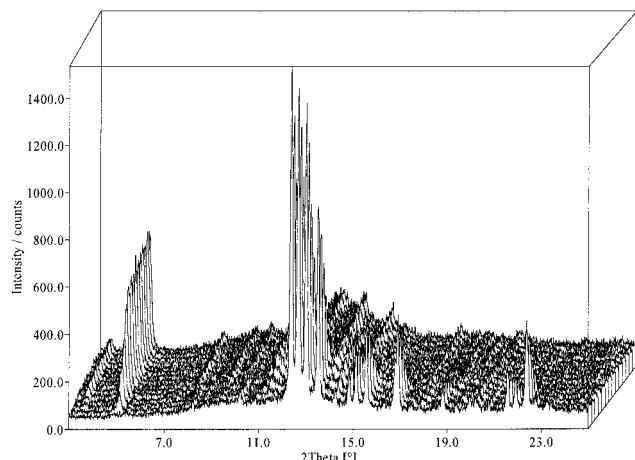


Figure 7. X-ray thermodiffractometric powder patterns of the phase transition of $\beta\text{-NaC}_2\text{N}_3$ (**1b**) to $\text{Na}_3\text{C}_6\text{N}_9$ (**2**) (300–450 °C, steps 10 °C, from the front to the rear).

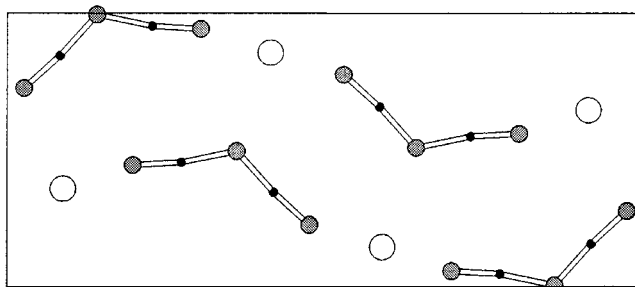


Figure 8. Crystal structure of $\alpha\text{-NaC}_2\text{N}_3$ (**1a**) (view along [001]) [Na: open circles, C: black circles, N: gray circles].

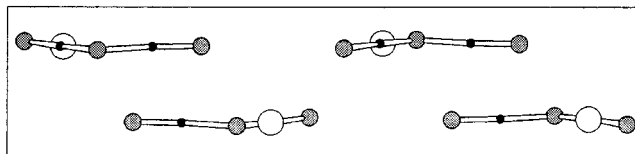


Figure 9. Crystal structure of $\alpha\text{-NaC}_2\text{N}_3$ (**1a**) (view along [100]) [Na: open circles, C: black circles, N: gray circles].

Table 2. Atomic Coordinates and Displacement Factors [pm²] for $\alpha\text{-NaC}_2\text{N}_3$ (**1a**) and $\beta\text{-NaC}_2\text{N}_3$ (**1b**) (First and Second Line, Respectively)

atom	Wyckoff position	x	y	z	U_{iso}^a
Na	4e	0.6437(3)	0.0878(1)	0.2606(8)	37(1)
	4c	0.648(1)	0.0867(3)	1/4	80(2)
C1	4e	0.1558(8)	0.0832(4)	0.2593(17)	31(2)
	4c	0.134(2)	0.0883(9)	1/4	30(4)
C2	4e	0.0468(7)	0.2269(4)	0.2623(19)	53(2)
	4c	0.054(2)	0.2323(10)	1/4	23(5)
N1	4e	0.2747(5)	0.0269(2)	0.2267(14)	31(2)
	4c	0.268(1)	0.0286(7)	1/4	17(4)
N2	4e	0.0056(5)	0.1410(3)	0.2840(13)	40(2)
	4c	0.007(2)	0.1493(10)	1/4	54(5)
N3	4e	0.0570(6)	0.3030(2)	0.2573(15)	44(2)
	4c	0.057(2)	0.3076(8)	1/4	43(5)

^a U_{iso} is defined as $\exp(-8\pi^2 U_{\text{iso}} \sin^2 \theta/\lambda)$.

(131 pm) than those to the terminal N atoms (114, 115 pm), representing single and triple bonds, respectively, as could be derived from the IR data.⁴ The N–C–N angles are almost linear (171°, 174°), whereas the C–N–C angle is 119° (Table 3). The anion is bent exhibiting approximately the point symmetry C_{2v} .

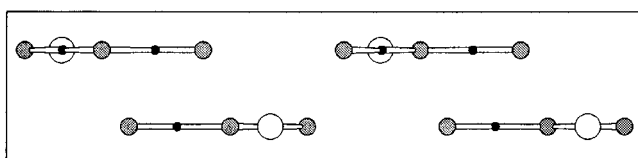


Figure 10. Crystal structure of $\beta\text{-NaC}_2\text{N}_3$ (**1b**) (view along [100]) [Na: open circles, C: black circles, N: gray circles].

The $\text{N}(\text{CN})_2^-$ ion is isoelectronic to the molecule N_3CN^{15} and to the recently described cationic species N_5^+ and $\text{N}(\text{CO})_2^+$.^{16,17}

The Na^+ are coordinated by six N atoms in the shape of an irregular octahedron. Five of these N atoms are terminal, whereas one N atom is bridging. Na^+ is coordinated by two N atoms of the same sheet and two of the sheets above and below this sheet, respectively. In this way it connects the $\text{N}(\text{CN})_2^-$ ions of different sheets.

The space group of **1b** (*Pbnm*) is a maximal nonisomorphic supergroup of *P2₁/n*, the space group of the low-temperature phase **1a**. The crystal structures of **1a** and **1b** are very similar, but in **1b** all atoms are positioned at the special Wyckoff positions with $y = 1/4$, and therefore the molecules are oriented exactly parallel to the plane (010) (Figure 10). The observed bond distances show a small deviation from the expected distances, because the measurement at higher temperature was taken within a shorter measuring time. Similar lattice constants and the same space group as in **1b** are found in the orthorhombic modification of AgC_2N_3 ,¹⁸ however, both compounds are not isotypic. In AgC_2N_3 the $\text{N}(\text{CN})_2^-$ ions are connected by Ag^+ in a different way, resulting in $\text{Ag}^+-\text{N}(\text{CN})_2^-$ chains. Ag^+ is coordinated by four terminal and by two bridging N atoms.

The temperature-dependent powder diffraction experiments document the phase transitions of NaC_2N_3 . Between 32 and 34 °C there is a change from monoclinic to orthorhombic crystal symmetry. Therefore the $h\bar{k}\bar{l}$ and hkl reflections of the monoclinic phase approach to each other and above 33 °C these reflections merge. The $0kl$ and $hk0$ reflections do not change during the phase transition. Slightly above the phase transition temperature all hkl reflections except $0kl$ and $hk0$ are rather broad, indicating strain inside the crystallites, but they become smaller with increasing temperature. The phase transition of **1a** to **1b** is a displacive one, because only small distortions of the atomic coordinates are necessary to yield the high-temperature phase. As the DSC data show, the phase transition is reversible with only a small hysteresis (Figure 1).

Despite the complex structure of **2** (54 positional parameters) its crystal structure determination from powder diffraction data by direct methods was successful. The lattice constants could be determined by conventional powder diffraction data, but the crystal structure determination was possible only with high-resolution synchrotron diffraction data.

In **2** there are tricyanomelamine ions $\text{C}_6\text{N}_9^{3-}$, which are connected by Na^+ cations (Figure 11). The anion consists of a triazine ring with three NCN sidearms connected to each C atom of the ring. There is no 3-fold symmetry of the anion as was found in $\text{Na}_3\text{C}_6\text{N}_9 \cdot 3\text{H}_2\text{O}$ or in the isoelectronic 2,4,6-triazido-1,3,5-triazine,¹⁹ because one of the sidearms is turned (point symmetry of the molecular ion C_s). This constitution of the arms

(15) Shurvell, H. F.; Hyslop, D. W. *J. Chem. Phys.* **1970**, 52, 881.

(16) Christe, K. O.; Wilson, W. W.; Sheehy, J. A.; Boatz, J. A. *Angew. Chem. Int. Ed.* **1999**, 38, 2004.

(17) Bernhardi, I.; Drews, T.; Seppelt, K. *Angew. Chem. Int. Ed.* **1999**, 38, 2232.

(18) Britton, D. *Acta Crystallogr.* **1990**, C46, 2297.

(19) Kessenich, E.; Klapötke, T. M.; Knizek, J.; Nöth, H.; Schulz, A. *Eur. J. Inorg. Chem.* **1998**, 2013.

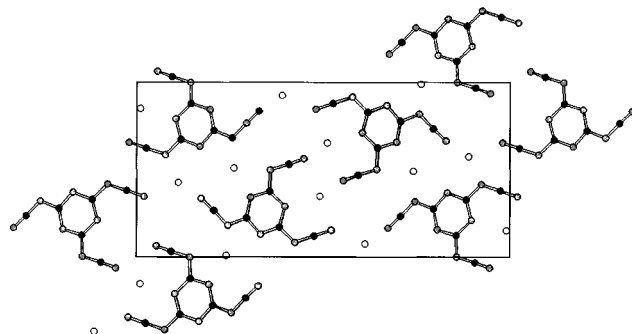


Figure 11. Crystal structure of $\text{Na}_3\text{C}_6\text{N}_9$ (**2**) (view along [001]) [Na: open circles, C: black circles, N: gray circles].

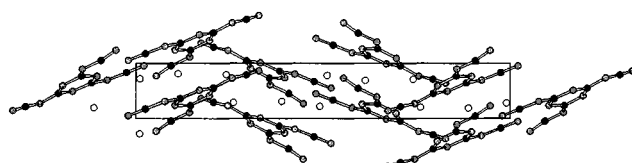


Figure 12. Crystal structure of $\text{Na}_3\text{C}_6\text{N}_9$ (**2**) (view along [100]) [Na: open circles, C: black circles, N: gray circles].

Table 3. Bond Lengths [pm] and Angles [$^\circ$] for α - NaC_2N_3 (**1a**) and β - NaC_2N_3 (**1b**)

	1a (22 $^\circ\text{C}$)	1b (150 $^\circ\text{C}$)
Na–N1	255.2(3)	261.8(9)
Na–N1	252.4(5)	255.3(8) 2 \times
Na–N1	254.3(5)	
Na–N2	247.0(4)	251.8(12)
Na–N3	246.9(5)	246.9(9) 2 \times
Na–N3	250.2(5)	
C1–N1	115.1(6)	124.8(12)
C1–N2	130.7(6)	122.8(13)
C2–N2	131.4(6)	127.8(15)
C2–N3	113.9(5)	112.6(13)
C1–N2–C2	119.2(5)	124(2)
N1–C1–N2	173.9(7)	178(21)
N2–C2–N3	171.1(6)	167(16)

was also found in hydrogen tricyanomelamines $\text{M}(\text{HC}_6\text{N}_9) \cdot 3\text{H}_2\text{O}$ ($\text{M} = \text{Co, Ni, Cu, Cd}$)²⁰ and in $\text{Co}(\text{H}_2\text{C}_6\text{N}_9)_2 \cdot 10\text{H}_2\text{O}$.²¹ The molecular ions are approximately planar and not arranged parallel to each other, but they tilt in different directions (Figure 12).

There are three differently coordinated Na^+ ions: Na1 and Na2 are connected to six N atoms and Na3 to seven N atoms. The distances Na–N vary from 237 to 289 pm (Tables 4, 5).

While in $\text{Na}_3\text{C}_6\text{N}_9 \cdot 3\text{H}_2\text{O}$ the N atoms of the triazine ring only build up hydrogen bonds to H_2O , in **2** both the N atoms of the triazine ring and those of the sidearms belong to the coordination spheres of the Na^+ .

The distances C–N range from 131 to 142 pm, except those to the terminal nitrogen (C–N: 113–121 pm) representing triple bonds. The distances and angles in $\text{Na}_3\text{C}_6\text{N}_9 \cdot 3\text{H}_2\text{O}$ and in the hydrogen tricyanomelamines are similar, although they show smaller variations due to the higher accuracy of the single-crystal structure refinement.

In contrast to the α - to β - NaC_2N_3 transformation, the phase transition of the monomer **1b** to the trimer **2** (>340 $^\circ\text{C}$) is a reconstructive one, because new bonds are built up to form the cyclic anion. The structure does not change when the phase is

Table 4. Atomic Coordinates and Displacement Factors [pm 2] for $\text{Na}_3\text{C}_6\text{N}_9$ (**2**)

atom	<i>x</i>	<i>y</i>	<i>z</i>	<i>U</i> _{iso} ^a
Na1	−0.4254(5)	−0.1117(3)	0.810(2)	382(23)
Na2	−0.1518(5)	0.0099(3)	1.280(2)	340(23)
Na3	0.0095(5)	0.2402(3)	0.207(2)	340(22)
C1	−0.1228(11)	0.1439(6)	0.769(4)	69(19)
C2	−0.3265(12)	0.1185(5)	0.640(4)	69(19)
C3	−0.2764(12)	0.2053(5)	0.453(4)	69(19)
C4	0.0324(11)	0.0928(5)	1.046(4)	69(19)
C5	−0.3780(10)	0.0257(5)	0.829(4)	69(19)
C6	−0.2313(11)	0.2937(6)	0.212(4)	69(19)
N1	−0.2090(11)	0.1029(4)	0.765(3)	167(14)
N2	−0.3698(9)	0.1686(5)	0.489(3)	167(14)
N3	−0.1571(10)	0.1947(5)	0.592(3)	167(14)
N4	−0.0008(10)	0.1426(4)	0.892(3)	167(14)
N5	−0.4162(9)	0.0770(4)	0.692(3)	167(14)
N6	−0.3189(9)	0.2563(5)	0.266(3)	167(14)
N7	0.0626(9)	0.0531(4)	1.231(3)	167(14)
N8	−0.3457(9)	−0.0208(4)	0.952(3)	167(14)
N9	−0.1656(9)	0.3275(4)	0.136(3)	167(14)

^a U_{iso} is defined as $\exp(-8\pi^2 U_{\text{iso}} \sin^2 \theta/\lambda)$; the displacement factors of C and N, respectively, were constrained to be equal.

Table 5. Bond Lengths [pm] and Angles [$^\circ$] for $\text{Na}_3\text{C}_6\text{N}_9$ (**2**); C1–C3 and N1–N3 Belong to the Triazine Ring, N4–N6 and C4–C6 Form the Side Arms, and N7–N9 Are Terminal

Na1–N2	270.9(12)	Na3–N2	268.2(12)
Na1–N5	244.6(11)	Na3–N3	284.5(13)
Na1–N5	276.2(11)	Na3–N3	265.4(12)
Na1–N8	232.8(11)	Na3–N4	253.3(11)
Na1–N9	243.5(11)	Na3–N6	260.9(11)
Na1–N9	250.8(11)	Na3–N6	253.9(11)
		Na3–N9	279.9(12)
Na2–N1	284.4(12)		
Na2–N1	288.5(12)		
Na2–N7	260.3(10)		
Na2–N7	261.9(12)		
Na2–N7	237.4(11)	N1–C1–N3	117.4(12)
Na2–N8	239.9(10)	N1–C1–N4	131.0(14)
		N3–C1–N4	111.4(11)
C1–N1	135.0(9)	N1–C2–N2	129.2(12)
C1–N3	137.0(10)	N1–C2–N5	115.2(12)
C1–N4	135.8(10)	N2–C2–N5	115.5(13)
C2–N1	136.2(9)	N2–C3–N3	124.0(11)
C2–N2	134.5(10)	N2–C3–N6	111.7(12)
C2–N5	141.7(10)	N3–C3–N6	124.3(13)
C3–N2	136.1(10)	N4–C4–N7	170.2(19)
C3–N3	136.4(10)	N5–C5–N8	178.8(14)
C3–N6	141.0(10)	N6–C6–N9	172.9(17)
C4–N4	131.4(9)	C1–N1–C2	116.9(12)
C4–N7	115.5(10)	C2–N2–C3	110.6(10)
C5–N5	133.9(9)	C1–N3–C3	120.9(11)
C5–N8	120.6(9)	C1–N4–C4	111.0(12)
C6–N6	133.7(9)	C2–N5–C5	118.0(12)
C6–N9	112.9(10)	C3–N6–C6	114.8(13)

cooled to room temperature, so the transition is irreversible (Figure 2). During heating there are reflections which belong either to **1b** or to **2** (Figure 7). At no temperature the sample is X-ray amorphous. Apparently the trimerization occurs directly in the solid-state without melting and without intermediates such as the dimer $\text{C}_4\text{N}_6^{2-}$.

With regard to the crystal structures of β - NaC_2N_3 and $\text{Na}_3\text{C}_6\text{N}_9$, it is obvious that there is no preorientation of the dicyanamide ions in the solid before the formation of the tricyanomelamine ring system. Solid-state NMR studies are planned to clarify the question of the mobility of $\text{N}(\text{CN})_2^-$ ions in the solid during the transition from **1b** to **2**.

Acknowledgment. Financial support by the Fonds der Chemischen Industrie, the Bundesministerium für Bildung und

(20) Abrahams, B. F.; Egan, S. J.; Hoskins, B. F.; Robson, R. *Chem. Commun.* **1996**, 1099.

(21) Abrahams, B. F.; Egan, S. J.; Hoskins, B. F.; Robson, R. *Acta Crystallogr.* **1996**, C52, 2427.

Forschung and the Deutsche Forschungsgemeinschaft (Gottfried-Wilhelm-Leibniz-Programm) as well as the ESRF (Grenoble) is gratefully acknowledged. The authors thank Drs. H. Emerich, K. Knudsen, and W. van Beek (ESRF) for their help during the synchrotron experiment.

Supporting Information Available: A table of indices, *d*-values, observed and calculated square structure factors from the Rietveld refinements of α -NaC₂N₃, β -NaC₂N₃, and Na₃C₆N₉. This material is available free of charge via the Internet at <http://pubs.acs.org>.

IC991044F